Hindawi
Journal of Sensors
Volume 2019, Article ID 8285240, 8 pages
https://doi.org/10.1155/2019/8285240

Review Article

Application Topics of Amorphous Wire CMOS IC Magneto-Impedance Micromagnetic Sensors for I-o-T Smart Society

Kaneo Mohri,[1] **Michiharu Yamamoto**,[2] **and Tsuyoshi Uchiyama**[3]

[1]*Nagoya Industrial Science Research Institute, Nagoya 464-0819, Japan*
[2]*Aichi Steel Corp., Arao-machi, Tokai 476-8666, Japan*
[3]*Grad. School of Eng., Nagoya Univ., Nagoya 464-8603, Japan*

Correspondence should be addressed to Kaneo Mohri; mohri@nisri.jp

Received 22 November 2018; Accepted 15 May 2019; Published 11 November 2019

Academic Editor: Vincenzo Stornelli

We proposed ten requisite conditions for successful development of wearable I-o-T smart magnetic sensors considering recent development of some successful micromagnetic sensors. We reported application topics using the amorphous wire CMOS IC magnetoimpedance micromagnetic sensor (MI sensor) on the geomagnetic field sensor for the electronic compass installed in the smartphones, the pitching ball self-spin analyzer installed in the professional baseball, self-driving magnetic guidance system, and the biomagnetic field sensing. Performances of the MI sensor overcoming the ten requisite conditions are discussed as a smart micromagnetic sensor on the basis of the magnetoimpedance effect in the amorphous wire.

1. Introduction

One of the most important target concepts of the sensors for the I-o-T smart society is so-called “Wearable,” in that the sensors must operate compensating the biosensory ability for the information tablet holder such as the direction sensing in unfamiliar places matching with the human personal daily behavior. For example, the smart magnetic sensors must completely recover to the original operating point even when the sensor happened to be exposed to a strong magnetic field generated from a strong magnet (the magnetic shock). Thus, we should recognize that requisite conditions for the wearable I-o-T smart sensors are quite different from that for conventional sensors mainly operated by trained engineers at special indoor places. Cooperation of the high-performance magnetic sensor device (hard ware) and the signal processing computer (soft wear) is also important for creation of the smart system.

2. Requisite Conditions for *Wearable* I-o-T Smart Magnetic Sensor

We should recognize the following ten requisite conditions for the successful development of wearable I-o-T smart magnetic sensors considering the recent development of some successful micromagnetic sensors:

(1) High sensitivity with high directivity: resolution 0.1 mG (10 nT) for the detection of the geomagnetic field (around ±500 mG range at Japan and around ±700 mG range at the pole area)

(2) High linearity with a wide dynamic range: around ±8 G (0.8 mT) for inside car box usage in stationary DC magnetic field disturbance and high directivity

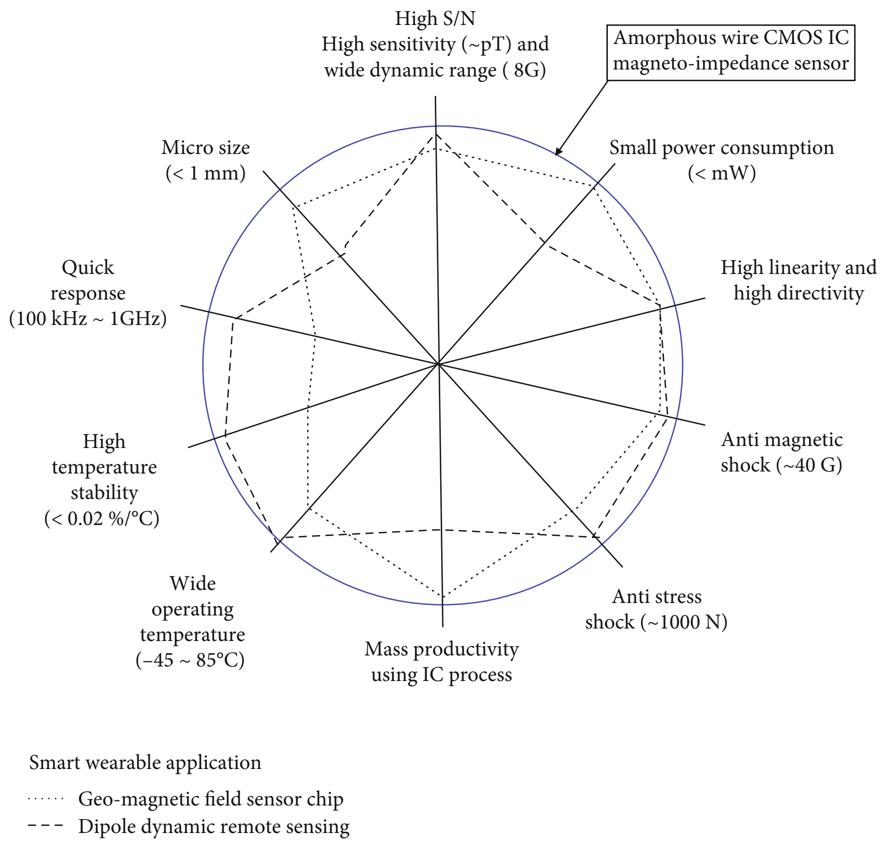

Figure 1: A map for the trial of detailed expression of the smart micromagnetic sensors based on recent successful application of the amorphous wire CMOS IC magnetoimpedance micromagnetic sensor that covers ten requisite conditions for the geomagnetic field sensing chip installed in the smartphone as the electronic compasses (short-dotted line) and the MI sensor module magnet marker guidance self-driving system (thick-dotted line).

(3) Antimagnetic shock with complete recovery to the original operating point for after exposure of around 40 G (4 mT) DC instantaneous disturbance magnetic field

(4) Quick response: around 100 kHz for the detection of a small magnetic field generated from small marker magnet set on the road in the magnet guidance self-driving system

(5) Microsizing: chip size less than 2 mm for installation in the smartphones

(6) Small power consumption: less than 0.3 mW for installation in the mobile phones

(7) High stability for temperature variation: less than 0.02%/°C output variation for sensor stationary use

(8) High operating temperature range: -40~+85°C for sensor outdoor usage in the world

(9) Antishock stresses: more than around 1000 N

(10) Mass productivity of high reliability chip using the integrated circuit technology for strict outdoor usage

We have tried to express in detail what is the smart sensor in the case of the micromagnetic sensors as in Figure 1 on the basis of recent successful applications of the amorphous wire and CMOS IC magneto-impedance sensor. The wearable sensors or smart sensors should overcome the comprehensive high-performance requisite conditions.

3. Amorphous Wire CMOS IC Magnetoimpedance Sensor

One of the most successful micromagnetic sensors overcoming the above-mentioned ten requisite conditions is the amorphous wire CMOS IC magnetoimpedance sensor (MI sensor) [1–17] on the basis of the following principal equations.

The impedance Z of an amorphous magnetic alloy wire is

$$Z = \frac{R_{dc} ka J_0(ka)}{2J_1(ka)},$$
$$R_{dc} = \frac{\rho \ell}{\pi a^2},$$
$$k = (1-j)\delta,$$
$$\delta = \left(\frac{2\rho}{\omega \mu (H_{ex})}\right)^{1/2}, \quad (1)$$

where α is the amorphous wire radius, δ is the skin depth, ρ is the resistivity of the amorphous wire (130 $\mu\Omega$ cm), ℓ is the amorphous wire length, J_0 and J_1 are the 0^{th} and 1^{th} Bessel's functions, and $\mu(H_{ex})$ is the maximum differential permeability along the circumferential direction, respectively.

When $\delta \ll a$ (strong skin effect; $\omega \gg 2\rho/\mu a^2$),

$$Z \fallingdotseq (1+j)\frac{\left(aR_{dc}\left(\omega\mu\left(H_{ex}\right)\right)\right)^{1/2}}{2(2\rho)^{1/2}} \quad \text{(magnetoimpedance effect)}. \tag{2}$$

The magnetoimpedance effect is based on the strong skin effect in the zero-magnetostrictive amorphous alloy wire rapidly quenched in a running water and then the cold drawn thin bulk material. The magnetization of the MI sensor is carried out by only the magnetization rotation in the surface layer having the easy magnetization along the wire circumferential direction by the application of the read out wire sharp current inducing the strong skin effect. The high impedance as shown in equation (2) makes it possible to create a microsized magnetic element operable in a sensor semiconductor circuit with a high signal to noise ratio (S/N) in the wide dynamic range [14], a high directivity, and quick response even up to 1 GHz. An induced pulse magnetic flux is detected at the pick-up coil resulting in the high linearity with the wide dynamic range in the magnetic field detection and a high antimagnetic shock in the magnetic sensing operation. Thus, the MI sensor overcomes the above-mentioned ten requisite conditions for the I-o-T smart sensors [13].

4. Electronic Compass

The electronic compass serves as the pedestrian navigation system in the smartphones and other mobile phones cooperated with the global positioning system (GPS). The electronic compass determines the horizontal direction with accurate sensing of the geomagnetic field using the three-dimensional (3D) micromagnetic sensor, while the GPS determines the position. The system serves a walking navigation for the holder with a map heading on the mobile phone display. The mobile phone angle against the horizontal plane is detected in a gravity acceleration sensor. The electronic compass installed in the mobile phones needs a high-performance 3D micromagnetic sensor with the ten requisite conditions although the response speed condition is rather flexible.

Figure 2 illustrates a photograph of an electronic compass chip of 2 mm long, 2 mm wide, and 1 mm thick produced by Aichi Steel Corp. in which 3D orthogonal amorphous wires of around 0.5 mm length are installed as the magnetic head of the MI sensor [15, 16].

Electronic compass chip for smartphone (2×2×1 mm)

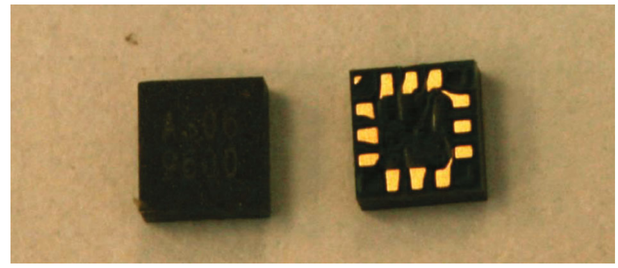

Figure 2: Amorphous wire CMOS IC MI sensor electronic compass chip (Aichi Steel Corp.).

5. Ball Spin Self-Analyzer

A ball spin self-analyzer for baseball pitching available for professional baseball players has been newly developed [18]. A MI sensor is installed in the official professional baseball (67 mm diameter and 140 gram weight) and detects the ball spin presently up to 50 rps utilizing the relatively detected data of the 3D geomagnetic field. Thus, the quick response speed performance and the antishock stress functions of the MI sensor are especially utilized with the microsizing and the high sensitivity of magnetic field detection. Conventionally, the speed, spin, and spin angle of a pitched ball are detected using the fixed camera system (Speed Gun). The self-spin analyzer needs the antishock ability compared with the camera system when the ball is caught at the catcher mitt. The data of a pitched ball is sent to the smartphone and smoothly displayed on the display with images and numerical values.

Figure 3 is an explanatory image for the cross section of a ball with an installed MI sensor.

6. Self-Driving Magnetic Guidance System

The self-driving or the autonomous driving is a new worldwide high technology project to create a civilian mobility infrastructure and promotes the intelligent transport system (ITS). The self-driving is composed of the stationary self-driving and the accidental self-driving. One of the most reliable stationary self-driving systems is the magnetic guidance system, in that magnetic sensors set to the underbody of a vehicle detect a magnetic field generated from a marker magnet moment set on the road surface-designed line. The magnetic field $H(r)$ generated from a magnetic moment at the magnetic sensor head has been known expressed as

$$H(r) = \left(\frac{-1}{4\pi\mu_o r^3}\right)\left(M_m - \left(\frac{3}{r^3}\right)(M_m r)r\right), \tag{3}$$

where M_m is the magnetic dipole moment of the marker magnet and r is the position vector between M_m and the sensor head position.

A trial of a magnetic guidance system named IMTS [19] has been carried out at the EXPO 2005 area for transport of attendees in buses without drivers using an exclusive road with a guidance marker of strong NdFeB magnets that needed high cost due to special treatment such as shielding against humidity. Magnetic fixing of magnetic things to the road marker strong magnets was also a problem for road maintenance trouble.

A new magnetic guidance system [20, 21] solved the above-mentioned high-cost problem of a strong road marker magnet using a combination of a sensitive MI sensor array module and a small low-cost SrO ferrite magnet marker.

Figure 3: Cross section of a baseball with installed MI sensor module.

The sensitive MI sensor detects not only a small marker signal magnetic field of several mG (nT) but also various larger disturbance magnetic fields of more than 100 mG on the road generated from road structure steels or bridge steels utilizing the wide sensing dynamic range of the MI sensor. Each MI sensor is designed as the differential type magnetic sensor, in which a pair of sensor head amorphous wires (6 mm long each) are aligned in parallel with 5 mm interval and set along the vehicle transport direction. The marker signal magnetic field only is determined by the differential type MI sensor output signal processing using the band pass filter in the magnetic sensor module of ten MI sensor arrays in the alignment of each 10 cm position interval set to the vehicle front underbody along the vehicle width direction (vertical direction to the road marker line) utilizing the magnetic field spatial distribution difference of wide distribution of the disturbance magnetic field while sharp distribution of the marker magnetic field generated from a cylindrical ferrite magnet of 3 cm diameter and 3.8 cm length set vertically at each 2 m position on the road along the designed driving line.

The differential type MI sensors do not detect the geomagnetic field, large (around 500 mG (50 μT) in Japan) but locally uniform, and the band pass filters finally eliminate all road ambient disturbance fields, locally broadly distributed around the marker during the running vehicle passing the small marker magnet (the magnetic field variation is at least 10 kHz for the running vehicle with a speed 100 km/h).

Thus, an accurate running of a test bus of less than 5 mm deflection on the running line regardless of the time and the weather conditions is resulted. Successful results with zero trouble have been obtained using the MI sensor module ferrite magnet marker magnetic guidance system through five verification tests managed by Japanese Government (Ministry of Land, Infrastructure, and Transport) in 2017-2018 years [22] even at a snowing area in Hokkaido mountain area [23]. The new magnetic guidance system using the MI sensor array module has successfully worked covering the inside of the tunnel area, snow area, and the airport area regardless of day and night times and weather conditions where the GPS is not available due to the electromagnetic wave problem [23].

Figure 4 represents a photograph of the test bus driving at a mountain area [24].

The differential type MI senor module (transverse train) and ferrite magnet marker guidance system is constituted with the following magnetic sensing and signal processing steps as illustrated in Figure 5 [25]:

Step 1. Accurate detection of all magnetic fields of a road surface marker magnet dipole and other various large disturbance magnetic fields generated from magnetic remanence of the road structure steels using sensitive, wide dynamic range and quick response MI sensor array

Step 2. Selection of the marker magnetic field among all magnetic fields using band pass filter signal processing electronic devices

Step 3. Determination of the marker position using the final signal processing software as shown in Figure 6

7. Biomagnetic Field Detection

The detection of human biomagnetic field is a challenge to create a new screening diagnosis technology combined with the electrocardiogram (ECG) especially for increasing number of blood circulation system diseases that is one of the basic information on health in so-called aged smart society. Human biomagnetic field on the blood circulation is detected using the pico-Tesla resolution MI sensor [11, 13]. Figure 7 illustrates the measured example of the biomagnetic field detected for five subjects at their left scapula bottom position in sitting attitude. Almost regular double peak waveform is recognized in the three healthy subjects of two males aged 54 and 46 and one female aged 73. These peaks are considered in correspondence to the open phase and the close phase of the aortic valve considering a phase relation to the simultaneously measured ECG [26]. While the double peak disappeared in the measured magnetic field waveform of two angina pectoris male patients aged 71 and 73. Thus, it is considered that biomagnetic field originated from the ion transition in blood vessel cells while the ECG reflected the activation potential at the heart muscle.

Figure 8 represents another biomagnetic field measurements using a pico-Tesla resolution MI sensor at the left scapula bottom position (Back-MCG) of a 28-year-old healthy man during sitting attitude before a magnetic stimulation

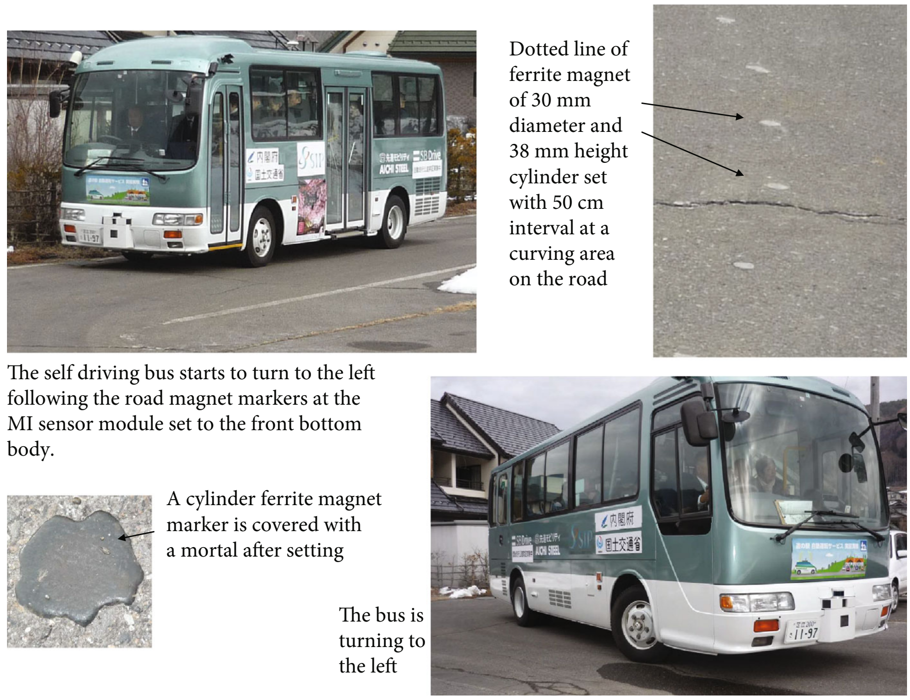

Figure 4: Verification test of a MI sensor magnetic guidance system self-driving bus at a mountain area.

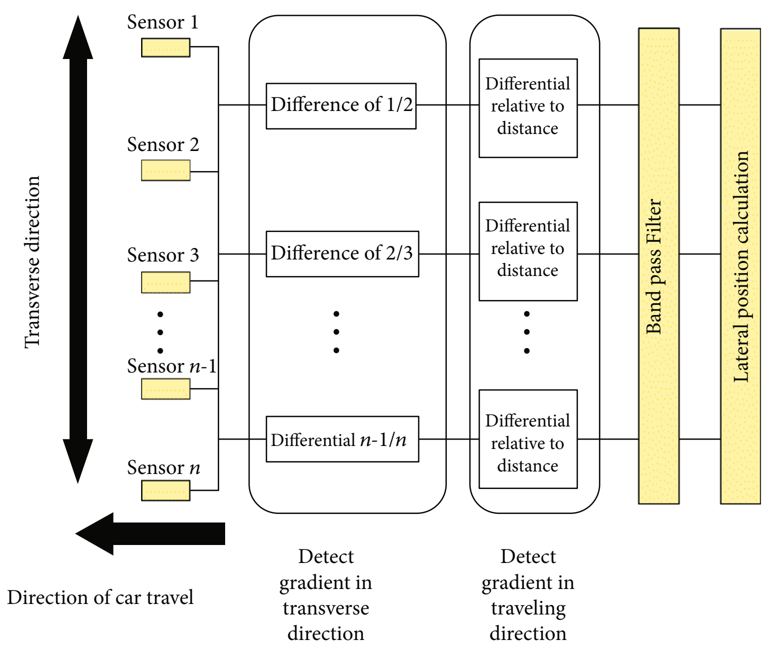

Figure 5: First, differential output is taken for 2 adjacent MI sensors apart at a 50 mm interval in a traverse direction and then amplified. In this step, most ambient magnetic noises including geomagnetic field is eliminated so that sufficient amplification would be possible. Then, the differentials relative to the car's traveling distance are taken. In this step, a particular marker pattern is distinguished, since a marker field has sharp up and down gradients, against the traveling distance. After the step, the signals are subjected to a band pass filter which is adjusted to the cycle in which the consecutive marker signals are coming in as the car travels forward. In the above manner, (N-1) output are obtained from N sensors. Then the peak value of each detected marker pattern is detected, and those (N-1) peaks are connected next to each other.

and after a magnetic stimulation with the application of 1-21 Hz, 100 mG, 4 ms pulse train magnetic field that is generated using a 2 sec cyclic frequency sweep voltage function generator connected to a coil of 10 cm diameter and 50-turn winding. We recognize a regular Back-MCG waveform after the ELF magnetic stimulation [25, 27].

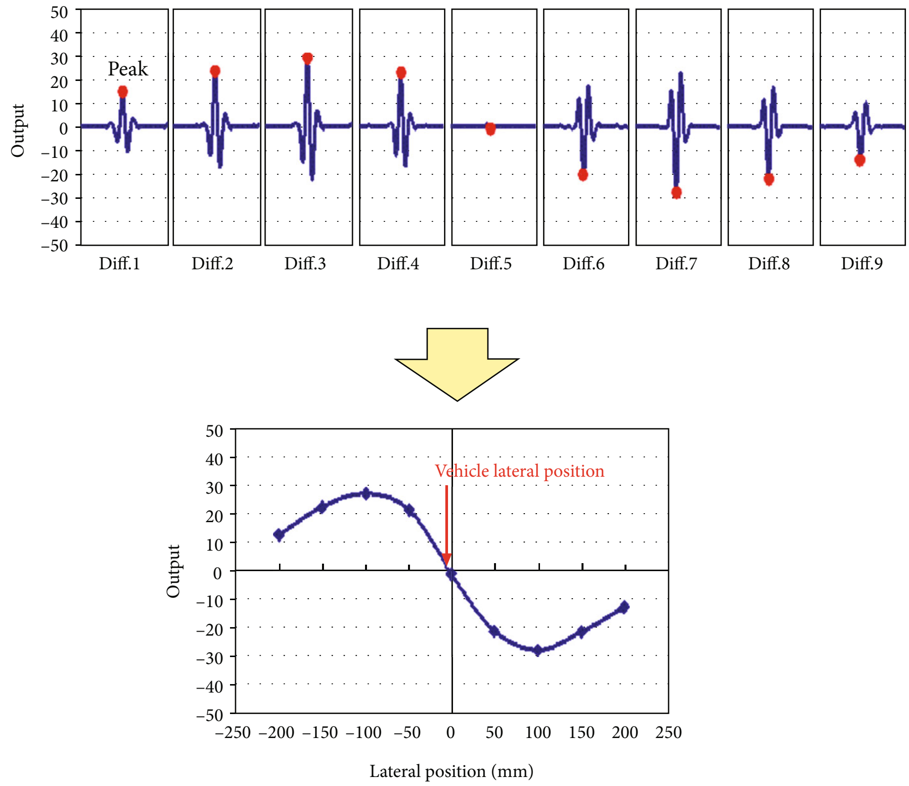

FIGURE 6: Since only one marker passes in sensor array at a time, the line of connected peaks will cross the zero field line, and the system determines the zero-cross point as the marker center. All these process are done in real time during vehicle travel.

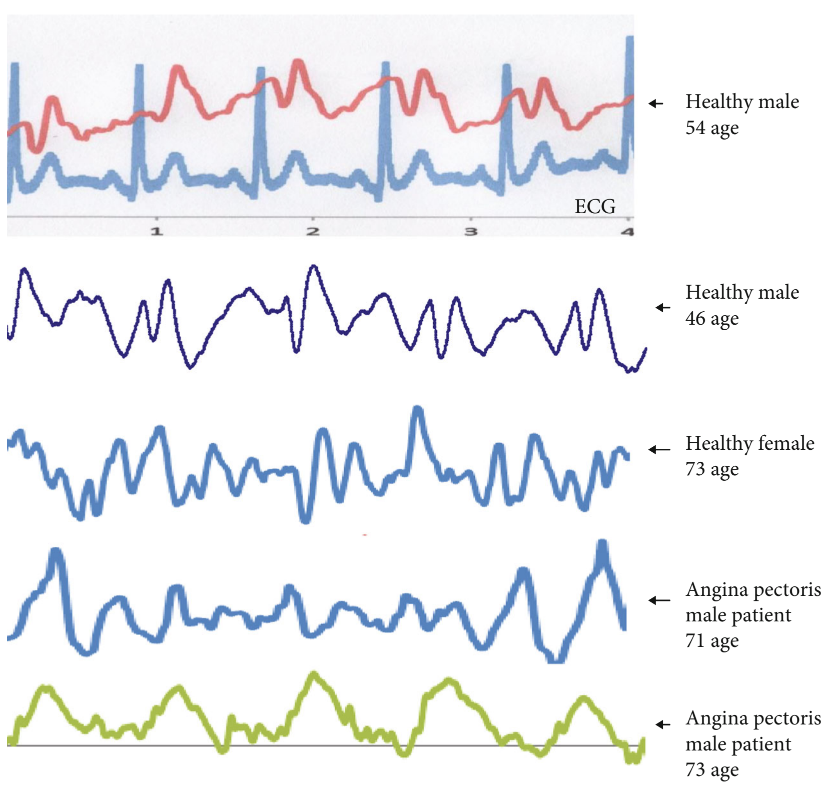

FIGURE 7: Measured magnetic field waveforms of 5 subjects at their left scapula bottom position during sitting attitude using a pico-Tesla resolution MI sensor.

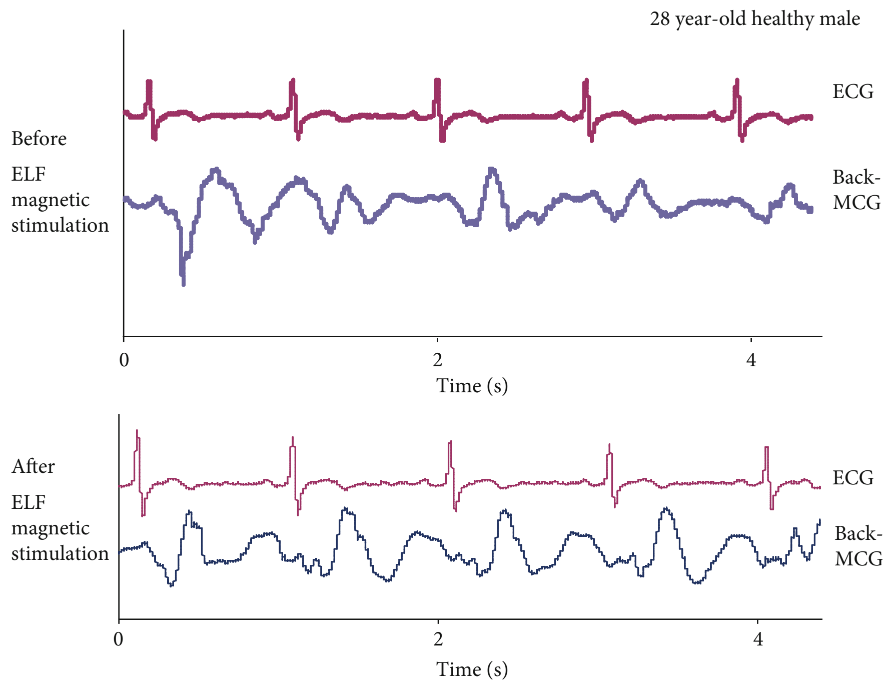

Figure 8: On time, measured results of the back magnetocardiogram (Back-MCG) using a pico-Tesla resolution MI sensor set close to the left scapula bottom position of a 28-year-old healthy man during sitting attitude before a magnetic stimulation and after a magnetic stimulation with the application of 1-21 Hz, 100 mG, 4 ms pulse train magnetic field on the spine position in 30 min. Electrocardiogram (ECG) was simultaneously detected.

The physiological bioactivation engineering not accompanied with the side effect is one of the biggest targets in the coming smart society. The magnetoprotonics is a theoretical magnetic bioactivation engineering based on the ATP physiology for increasing the proton mobility in the mitochondrial electron transport enzyme chain with perturbation of the water clusters $H^{+}{}_{3}O\ (H_2O)_n$, where $n = 1, 2, \cdots, n$, by the application of a small magnetic field having frequencies $f_n = qB_{dc}/2\pi m_n$, where q is the proton charge, B_{dc} is the geomagnetic field, m_n is the water cluster mass (in MKS unit), and $f_n = 1$–21 Hz in Japan. One of the useful verifications of the magnetoprotonics is the prevention of the car driver's drowsy driving without so-called "sleep rebound" [28] and decreasing the driving fatigue.

8. Conclusions

The I-o-T smart society is a target for the creation of a sustainable security society in that citizens anytime utilize various wearable sensors compensating their biosensory ability for avoidance of various dangers or inconveniences. Therefore, we must develop sufficiently reliable high-performance magnetic sensors overcoming at least the ten proposed requisite conditions. We reported application topics using the MI sensors due to relatively advantageous features among magnetic sensors.

Thus, we may define the smart magnetic sensor as the comprehensive multifunctional high-performance micromagnetic sensor operable anytime even wearable outdoor as a sports wrist watch.

9. Discussions

Some close and flexible collaboration among three technologies of (1) the materialization, (2) the magnetic effects, and (3) the magnetic sensor circuitry is necessary to create the smart micromagnetic sensor.

(I) The materialization on the magnetic materials shows small values of the magnetic anisotropy, K_u, sensitive magnetization rotation permeability, μ_r, and the demagnetizing field, H_{dem}, on the basis of material robustness with high elasticity and high tensile strength and also anticorrosiveness. For that, zero-magnetostrictive thin amorphous wires of Co-rich $(FeCo)_{80}(SiB)_{20}$ (at %) have been selected. The amorphous magnetic alloys show small K_u due to the noncrystalline structure resulting high μ_r. The amorphous wires show zero H_{dem} along the circumferential direction as used in the magnetoimpedance effect. The higher electric resistivity ρ of around 130 μm cm in the amorphous alloy wires is useful to construct a microsized magnetic head with a high impedance in the micromagnetic sensor electronic circuits

(II) Only the high-performance electromagnetic effects developed with the high-performance magnetic materials such as the zero-magnetostrictive amorphous wires create the smart micromagnetic sensors with ten functions overcoming the above-mentioned ten requisite conditions. The magneto-impedance effect in the zero-magnetostrictive amorphous wires is one of the high-performance magnetic effects expressed in equation (2), has created a smart micromagnetic sensor, and has spread the basic researches and developments not only the above application topics

(III) The smart micromagnetic sensors are mass-produced using the integrated circuit technology, in that the sensor circuit operation is based on the digital operation. Thus, the MI sensor operates with the pulse magnetoimpedance effect, in that a strong skin effect is generated with a sharp high-amplitude pulse current at the readout process [13]

Conflicts of Interest

The authors declare that they have no conflicts of interest.

References

[1] K. Mohri, M. Yamamoto, and H. Aoyama, "High-performance micro magnetic sensors installed in electronic compasses and I-o-T magnetic sensors promoting new information society – amorphous wire CMOS IC magneto-impedance sensors -," in *2018 IEEE International Magnetics Conference (INTERMAG)*, Singapore, April 2018 (BH-07).

[2] K. Mohri, "Application of amorphous magnetic wires to computer peripherals," *Materials Science and Engineering: A*, vol. 185, no. 1-2, pp. 141–145, 1994.

[3] L. V. Panina and K. Mohri, "Magneto-impedance effect in amorphous wires," *Applied Physics Letters*, vol. 65, no. 9, pp. 1189–1191, 1994.

[4] K. Mohri and Y. Honkura, "Amorphous wire and CMOS IC based magneto-impedance sensors–origin, topics, and future," *Sensor Letters*, vol. 5, no. 1, pp. 267–270, 2007.

[5] T. Kanno, K. Mohri, T. Yagi, T. Uchiyama, and L. P. Shen, "Amorphous wire MI micro sensor using C-MOS IC multivibrator," *IEEE Transactions on Magnetics*, vol. 33, no. 5, pp. 3358–3360, 1997.

[6] K. Mohri, T. Uchiyama, and L. V. Panina, "Recent advances of micro magnetic sensors and sensing application," *Sensors and Actuators A*, vol. 59, no. 1-3, pp. 1–8, 1997.

[7] N. Kawajiri, M. Nakabayashi, C. M. Cai, K. Mohri, and T. Uchiyama, "Highly stable MI micro sensor using CMOS IC multivibrator with synchronous rectification [for automobile control application]," *IEEE Transactions on Magnetics*, vol. 35, no. 5, pp. 3667–3669, 1999.

[8] K. Mohri, T. Uchiyama, L. P. Shen et al., "Amorphous wire and CMOS IC-based sensitive micro magnetic sensors utilizing magnetoimpedance (MI) and stress-impedance (SI) effects," *IEEE Transactions on Magnetics*, vol. 38, no. 5, pp. 3063–3068, 2002.

[9] K. Mohri, F. B. Humphrey, L. V. Panina et al., "Advances of amorphous wire magnetics over 27 years," *Physica Status Solidi A: Applications and Materials Science*, vol. 206, no. 4, pp. 601–607, 2009.

[10] T. Uchiyama, K. Mohri, and S. Nakayama, "Measurement of spontaneous oscillatory magnetic field of guinea-pig smooth muscle preparation using pico-tesla resolution amorphous wire magneto-impedance sensor," *IEEE Transactions on Magnetics*, vol. 47, no. 10, pp. 3070–3073, 2011.

[11] T. Uchiyama, K. Mohri, Y. Honkura, and L. V. Panina, "Recent advances of pico-Tesla resolution magneto-impedance sensor based on amorphous wire CMOS IC MI sensor," *IEEE Transactions on Magnetics*, vol. 48, no. 11, pp. 3833–3839, 2012.

[12] K. Mohri, Y. Honkura, L. V. Panina, and T. Uchiyama, "Super MI sensor: recent advances of amorphous wire and CMOS-IC magneto-impedance sensor," *Journal of Nanoscience and Nanotechnology*, vol. 12, no. 9, pp. 7491–7495, 2012.

[13] K. Mohri, T. Uchiyama, L. V. Panina, M. Yamamoto, and K. Bushida, "Recent advances of amorphous wire CMOS IC magneto-impedance sensors; innovative high-performance micromagnetic sensor chip," *Journal of Sensors*, vol. 2015, Article ID 718069, 8 pages, 2015.

[14] L. G. C. Melo, D. Ménard, A. Yelon, L. Ding, S. Saez, and C. Dolabdjian, "Optimization of the magnetic noise and sensitivity of giant magnetoimpedance sensors," *Journal of Applied Physics*, vol. 103, no. 3, pp. 33903–3303-6, 2008.

[15] Y. Kotani, M. Yamamoto, and Y. Honkura, *The development of amorphous wire MI sensor for car use*, All Toyota Research Workshop, 2002.

[16] C. M. Cai, T. Nagao, M. Mori, and M. Yamamoto, *The development of super compact electronic compass for smartphone use*, All Toyota Research Workshop, 2010.

[17] L. V. Panina, "Magnetoimpedance (MI) in amorphous wires; new materials and applications," *Physica Status Solidi A: Applications and Materials Science*, vol. 206, no. 4, pp. 656–662, 2009.

[18] https://www.mizuno.jp/baseball/products/MAQ/.

[19] http://www.expo2005.or.jp.

[20] https://www.aichi-steel.co.jp/news_item/20171211_topics.pdf.

[21] M. Yamamoto, T. Nagao, and H. Aoyama, "Ultra-low field magnetic guidance system," *Proceedings of the 23rd ITS World Congress, ITS-TP0082*, 2016, pp. 1–11, Melborne, October 2016.

[22] http://www.mlit.go.jp/common/001227121pdf.

[23] https://www.hkd.mlit.go.jp/ob/douro_keikaku/fns6a1000000cllt.html.

[24] http://www.nagano-np.co.jp/articles/39720.

[25] K. Mohri, T. Uchiyama, M. Yamada et al., "Physiological magnetic stimulation for arousal of elderly car driver evaluated with electro-encephalogram and spine magnetic field," *IEEE Transactions on Magnetics*, vol. 48, no. 11, pp. 3505–3508, 2012.

[26] H. Sugi, Ed., *Physiology of Human Body Function*, Nankodo, 1999.

[27] K. Mohri and M. Fukushima, "Milligauss magnetic field triggering reliable self-organization of water with long-range ordered proton transport through cyclotron resonance," *IEEE Transactions on Magnetics*, vol. 39, no. 5, pp. 3328–3330, 2003.

[28] M. Tsukada, S. Takegawa, T. Nakano, M. Yamada, and K. Mohri, "Study on improvement of driver arousal technique with physiological magnetic stimulation," in *Proceedings of the ITS AP Forum 2018*, pp. 215–224, Fukuoka, 2018.